Expression and characterization of the SOS1 Arabidopsis salt tolerance protein

Asad Ullah, Debajyoti Dutta & Larry Fliegel

Molecular and Cellular Biochemistry
An International Journal for Chemical Biology in Health and Disease

ISSN 0300-8177
Volume 415
Combined 1-2

Mol Cell Biochem (2016) 415:133-143
DOI 10.1007/s11010-016-2685-2

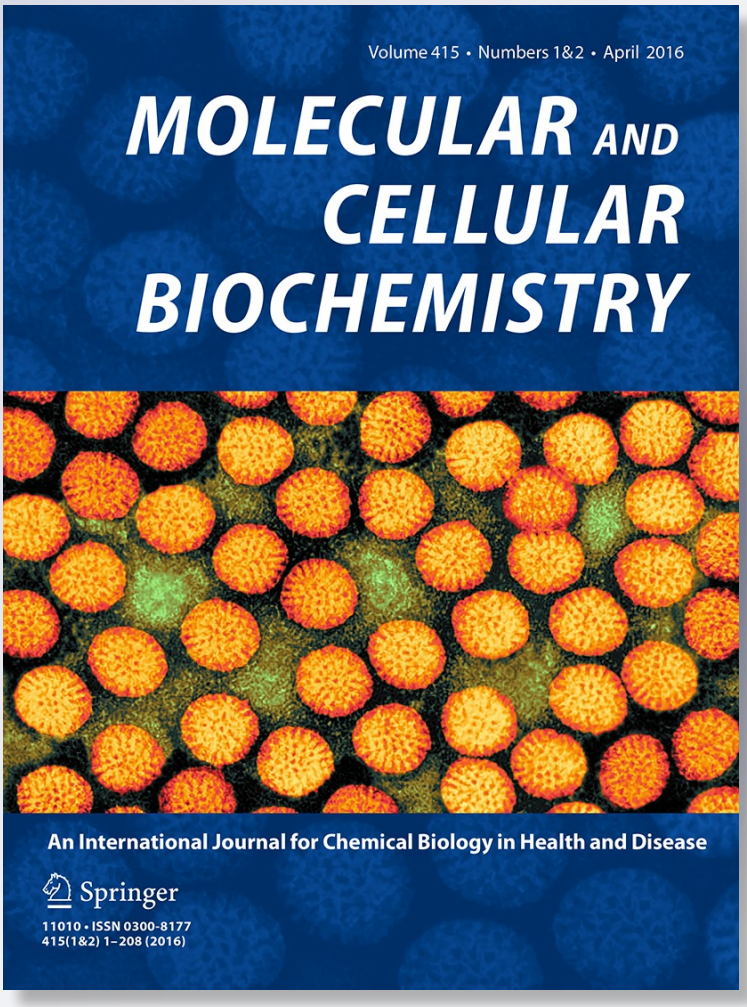

Springer

Mol Cell Biochem (2016) 415:133–143
DOI 10.1007/s11010-016-2685-2

Expression and characterization of the SOS1 Arabidopsis salt tolerance protein

Asad Ullah[1] · Debajyoti Dutta[1] · Larry Fliegel[1]

Received: 8 December 2015 / Accepted: 12 March 2016 / Published online: 18 March 2016

Abstract SOS1 is the plasma membrane Na^+/H^+ antiporter of *Arabidopsis thaliana.* It is responsible for the removal of intracellular sodium in exchange for an extracellular proton. SOS1 is composed of 1146 amino acids. Approximately 450 make the membrane domain, while the protein contains and a very large regulatory cytosolic domain of about 696 amino acids. *Schizosaccharomyces pombe* contains the salt tolerance Na^+/H^+ antiporter proteins sod2. We examined the ability of SOS1 to rescue salt tolerance in *S. pombe* with a knockout of the sod2 gene (sod2::ura4). In addition, we characterized the importance of the regulatory tail of SOS1, in expression of the protein in *S. pombe*. We expressed full-length SOS1 and SOS1 shortened at the C-terminus and ending at amino acids 766 (medium) and 481 (short). The short version of SOS1 conveyed salt tolerance to sod2::ura4 yeast and Western blotting revealed that the protein was present. The protein was also targeted to the plasma membrane. The medium and full-length SOS1 protein were partially degraded and were not as well expressed as the short version of SOS1. The SOS1 short protein was also able to reduce Na^+ content in *S. pombe*. The full-length SOS1 dimerized and depended on the presence of the cytosolic tail. An analysis of SOS1 predicted a topology of 13 transmembrane segments, distinct from *E. coli* NhaA but similar to the Na^+/H^+ exchangers *Methanocaldococcus jannaschii* NhaP1 and *Thermus thermophile* NapA.

✉ Larry Fliegel
lfliegel@ualberta.ca

[1] Department of Biochemistry, University of Alberta, 347, Medical Science Building, Edmonton, AB T6G 2H7, Canada

Keywords *Arabidopsis thaliana* · Membrane protein · Na^+/H^+ antiporter · Salt tolerance · Sod2 · SOS1

Introduction

Under normal physiological circumstances plants, yeast, and mammalian cells have relatively low Na^+ concentrations in their cytosol. These organisms respond to salt stress in several ways. One is by changing gene expression patterns that will minimize damage [1]. Another direct way that plants and yeast deal with excess "toxic" levels of intracellular Na^+ is to either extrude it, or to sequester it into vacuoles, thereby reducing the cytosolic concentration. In plants, varying types of plasma membrane Na^+/H^+ antiporters remove sodium. The energy of transport comes from the proton gradient generated by the plasma membrane H^+-ATPase or from the vacuolar H^+-ATPase and H^+-PPiase that generate a gradient across the vacuolar membrane [2]. Plant Na^+/H^+ antiporters have been isolated from a variety of sources including Arabidopsis [3, 4], rice [5], halophytic plants (*Atriplex*) [6], and *Mesembryanthemum crystallinum* [7]. One important type of Na^+/H^+ antiporter is the SOS1 (for salt overly sensitive type 1 mutant) type. This type of antiporter is a plasma membrane Na^+/H^+ antiporter with significant sequence similarity to Na^+/H^+ antiporters from bacteria and fungi. They play the most important role of the three types of SOS loci in plants [4]. Overexpression of SOS1 has been shown to improve salt tolerance in plants [8].

In yeast, transporters and other regulatory proteins mediate salt tolerance. In the fission yeast *Schizosaccharomyces pombe*, the Na^+/H^+ antiporter (sod2) plays the major role in salt removal from the cytosol and in salt tolerance [9]. Disruption of the sod2 gene results in a

reduced ability to extrude cytoplasmic Na^+ and to take up external protons in exchange for internal sodium ions [9]. Sod2 removes Na^+ or Li^+ from the cytosol at the expense of the proton gradient created by the plasma membrane ATPase [9, 10]. We have earlier [11, 12] used *S. pombe* with a knockout of the sod2 gene to study the effects of mutation of amino acids in this protein. Knockout of sod2 leads to a salt-sensitive growth phenotype in *S. pombe*.

Yeast and plant Na^+/H^+ antiporters are not identical but they share evolutionarily conserved functions and can substitute for one another functionally [13]. Importantly, sod2 of *S. pombe* has been shown to convey salt tolerance to *Arabidopsis* and can function as SOS1 at the plasma membrane [14]. SOS1 is evolutionarily related to sod2 and clusters with it in phylogenetic analysis [4]. It is also similar to sod2 in several key regions of the membrane-transporting domain (personal observation). In this study, we examined the ability of SOS1 to rescue salt tolerance in *S. pombe* with a knockout of the sod2 gene. In addition, we characterize the importance of the tail of SOS1 in this regard, and analyzed transmembrane segments of the protein and its predicted topology [15]. Our results show that SOS1 can rescue salt tolerance in *S. pombe* and demonstrate the importance of the tail in dimerization of the protein.

Materials and methods

Materials

Restriction enzymes were obtained from New England Biolabs, Inc. (Mississauga ON, Canada). PWO DNA polymerase was obtained from Roche Applied Science (Roche Molecular Biochemicals, Mannheim, Germany).

SOS1 sequence alignment and topology predictions

Arabidopsis thaliana SOS1 (atSOS1) topology was predicted by combining the results from multiple sequence alignment, secondary structure prediction, and transmembrane helix prediction. Multiple sequence alignment was performed using MAFFT [16]. *at*SOS1 was used to search for plant SOS1 homologs, *sp*Sod2 was used to find and include yeast, and fungi NHEs, *Ec*NhaA, and MjNhap1 (*Methanocaldococcus jannaschii*) were used to include bacterial and archeal NHEs, and human NHE1 was also included with the mammalian NHEs. Secondary structure prediction was done using two independent servers: psipred [17] and GOR V [18]. The common amino acid sequences belonging to similar secondary structures were selected to assign putative secondary structures. Hydrophobicity analysis was performed using TMHMM [19] and TMPred [20] servers.

Plasmid construction and site-directed mutagenesis

Full-length *Arabidopsis thaliana* SOS1 DNA was a generous gift from Dr. J.K. Zhu, Department of Botany and Plant Sciences, Institute for Integrative Genome Biology, University of California. SOS1 was cloned into the plasmid pREP41GFP, which has been described earlier [21] and contains a Gly–Ala linker preceding GFP. The GFP contains the Ser65Thr mutation and has an NdeI site removed by silent mutation. Three different constructs of SOS1 were made (pREP41SOSLGFP, pREP41SOSMGFP, pREP41SOSSGFP) with varying length of the large cytosolic tail. The largest was cloned into a NdeI site of pREP41GFP. The forward primer was SOS1f, 5′-aggccattaatatgacgactgtaatcgacg-3′ and contains an AseI for cloning that is compatible with NdeI. The reverse primer (SOS1L) 5′-cgcgcgattaattagatcgttcctgaaaacg-3′ was designed to remain in frame with the downstream GFP protein and produced a product that encoded for the entire 1146 amino acids of the SOS1 protein. Another construct used the same forward primer and a reverse primer (SOS1s, 5′-ggtcctagctcctcatcgtctcc-3′) for a PCR product of 1450 bp. This was digested with Ase I and Bgl II and cloned into the NdeI and Bam H1 sites of pREP41GFP. This short construct expressed amino acids 1-481 of SOS1 fused to GFP. A third construct of medium length used the reverse primer SOS1 m (5′-tgcgcgattaatgacaccacgcagtttcattggttc-3′) which contained an Ase I site for cloning. With the SOS1f primer it was designed to express an intermediate length protein, containing the first 766 amino acids of SOS1 fused to GFP.

Schizosaccharomyces pombe bearing the sod2 gene disruption (sod2::ura4) was used as a host for all transformations of yeast and were indicated as a control [11]. It was maintained on low sodium minimal KMA medium or yeast extract adenine (YEA) as described earlier [11, 12]. KMA medium contains (per 1 L): potassium hydrogen phthalate, 3 g; K_2HPO_4, 3 g; yeast nitrogen base without amino acids, 7 g; glucose, 20 g; and adenine, 200 mg. Leucine at 200 mg/l was added to maintain the *sod2::ura4 leu1-32* strain whenever appropriate and all media was buffered with 50 mM Mes/Citrate and adjusted to pH 5.0 with KOH. NaCl or LiCl was added to the media at the indicated concentrations to test for salt resistance wherever indicated. For growth curves 2×10^6 cells from an overnight exponentially growing culture were used to inoculate 2.5 ml of fresh media liquid and cultures were grown at 30 °C in a rotary shaker. At the times indicated, aliquots of cells were harvested and we determined the growth at A_{600}. All growth curves were determined in triplicate a minimum of three times. Growth on plates was supplemented with NaCl or LiCl at the indicated concentrations. The plasmid pREP-41sod2GFP has been described earlier [21] and contains full-length sod2 gene with a C-terminal GFP tag.

S. pombe transformed with the pREP-41sod2GFP plasmid grown in medium in the absence of thiamine, was used as a positive salt-resistant control.

Microscopy

Confocal imaging was performed on an Olympus IX81 microscope equipped with a Nipkow spinning disk optimized by Quorum Technologies (Guelph, ON, Canada). Images were acquired with the 100× objective on a Hamamatsu EM-CCD camera (Hamamatsu, Japan) using the software Volocity (Improvision Inc., Lexington, MA), and further processed in Adobe Photoshop. Yeast cells were fixed in 4 % formaldehyde prior to imaging.

SDS-PAGE and immunoblotting

Western blot analysis was used to examine expression of various SOS1 constructs [22]. Cell lysates were made from cultures of yeast transformed with various types of pREP41SOS1GFP. Yeast cells grown in KMA medium to an OD600 of 3 at 30 °C. Cells were pelleted (3500×*g*, 10 min) and washed with double-distilled water and resuspended in lysis buffer (50 mM Tris–HCl, pH 8.0, 5 mM EDTA), and a protease inhibitor cocktail(200 µM Pefabloc, 2 µg/mL Leuopeptin, 1 µg/mL Pepstatin, and 1 mM DTT) where indicated. They were then passed through an emulsiflex homogenizer at a pressure of 25,000 psi. Unbroken cells were removed by centrifugation at 3500×*g* for 5 min, and the supernatant was centrifuged at 14,000×*g* for 10 min. Enriched membranes of the supernatant were then were pelleted at 100,000×*g* for 1 h, and resuspended in small amount (200 µl) of buffer (50 mM Tris–HCl, pH 8, 5 mM EDTA and 1 mM DTT). They were quickly frozen in liquid nitrogen and stored at −80 °C. Equal amounts of up to 50 µg of each sample were resolved on a 10 % SDS/polyacrylamide gel. Nitrocellulose transfers were immunostained using a primary antibody of anti-GFP polyclonal antibody at a dilution of 1:10,000 (A generous gift of Dr. Luc Berthiaume, Dept. of Cell Biology, University of Alberta). Secondary antibody was IRDye 680-conjugated goat anti-rabbit polyclonal antibody (Bio/Can, Mississauga, ON, Canada) and the Odyssey® scanning system was used for Western detection (LI-COR Biosciences, USA).

Atomic absorption spectrophotometry

To determine the ability of wild-type and mutant sod2 proteins to remove intracellular Na^+ or Li^+, various strains were grown in KMA medium to an OD600 of approximately 0.4. Cells were harvested by centrifugation and washed and were then incubated in KMA medium supplemented with 100 mM NaCl for 1 h to load the cells with the cation. Cells were then harvested and were washed two times with 20 mM MES, pH 7.0, and resuspended in 10 ml buffer containing 20 mM MES pH 5.5, 0.1 mM $MgCl_2$, and 2 % glucose at 30 °C. Samples were taken at various intervals up to 2 h and Na^+ or Li^+ contents were determined by Atomic Absorption Spectrophotometry as described earlier [23]. Results are typical of three independent experiments.

Results

SOS1 topology analysis

Multiple distantly related sequences of NHEs are included in the sequence alignment to exploit the fact that minimal sequence similarity is retained among the NHE members (Fig. 1). Although these sequences are distantly related, the inclusive multiple sequence alignment results clearly identified transmembrane (TM) regions in atSOS1 and supports the known TM regions of bacterial NHE structures and the established human NHE1 topology [24, 25]. SOS1 is composed of 1146 amino acids. Residues 35–450 contain the transmembrane domain and 451–1146 are more hydrophilic and composed of a cytoplasmic regulatory domain. Our prediction of the more hydrophobic transmembrane domain suggests that SOS1 has 13 transmembrane helices. As the C-terminal regulatory domain is intracellular [26], residues 1–34 the first N-terminal residues, must be extracellular. The limits of the TM 1 segment are 36–54. The limits of TM 2 are 62–75. It has both strong helical prediction and high hydrophobicity score. The third TM segment spans from 100 to 114. This region has weak hydrophobicity score but strong helix prediction. The fourth TM segment consists of the residues 125–152. TM 5 is amino acids 160–180. TM 6 contains the residues 190–212. TM segments 7 and 8 include the residues 222–251 and 260–280, respectively where TM 7 has the highest hydrophobicity score.TM segment 9 is composed of the residues 285–296, which is the smallest of the TM helices. Residues from 311 to 335 belong to the TM segment 10. TM segment 11 is made up of the residues 353–377 while TM 12 is assigned to residues 388–408. TM segment 13 consists of residues 421–448. The proposed topology of SOS1, based on this analysis, is illustrated in Fig. 2.

Expression of SOS1 in *S. pombe*

We examined the ability of SOS1 to rescue salt tolerance in *S. pombe* that had a deletion of the major salt tolerance protein sod2. Several constructs of the SOS1 protein were

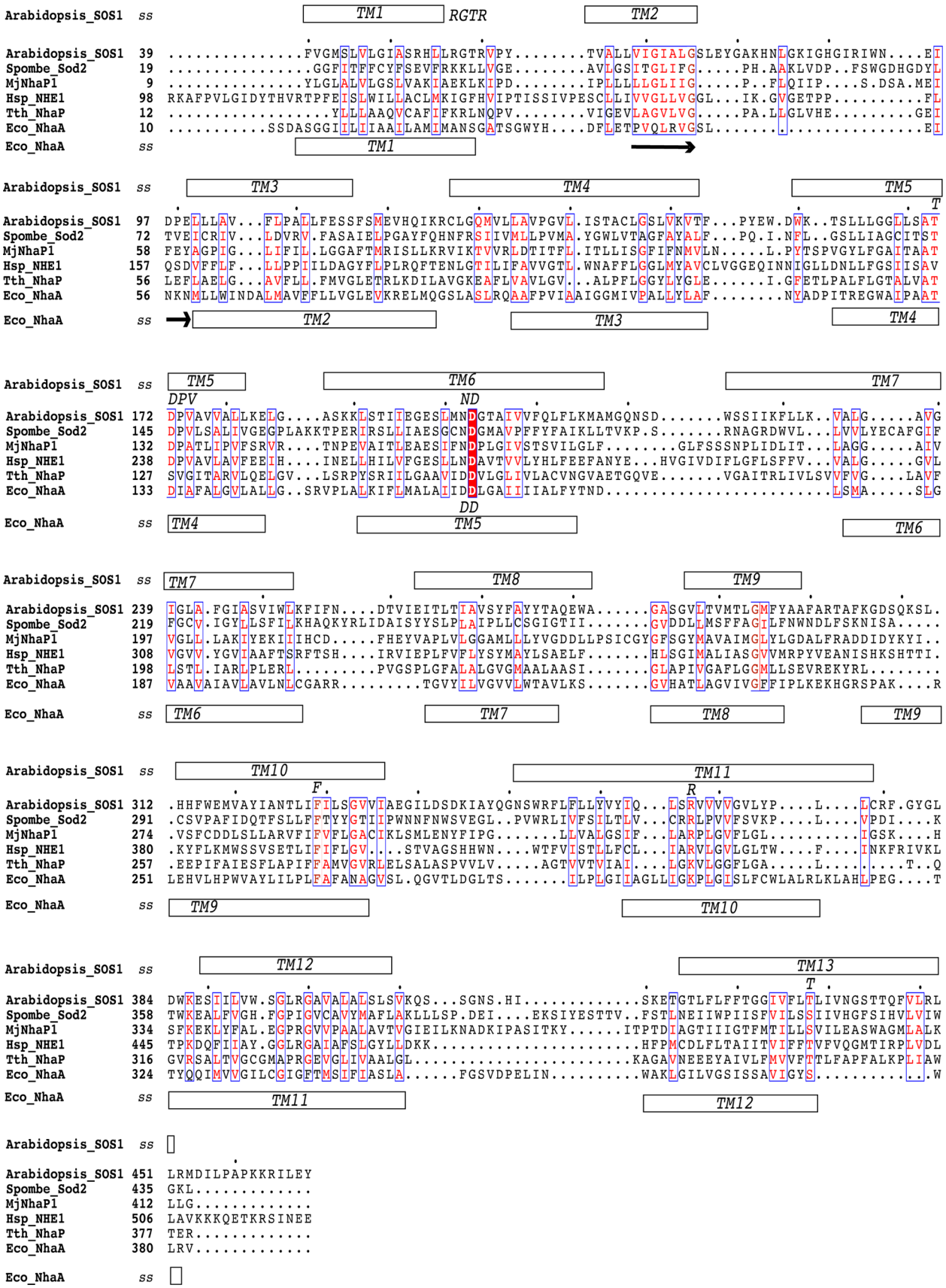

◀**Fig. 1** Structure-based sequence alignment of *at*SOS1 (*Arabidopsis*_SOS1) with several homologs. Spombe_Sod2 (*Schizosaccharomyces pombe* Sod2), MjNhaP1 (*Methanococcus jannaschii* NhaP1), Hsp_NHE1 (*Homo sapiens* NHE1), Tth_Nhap (*Thermus thermophilus* NhaP), Eco_NhaA (*Escherichia coli* NhaA). Predicted transmembrane segments of *at*SOS1 are depicted at the top and NhaA transmembrane segments are indicated at the lower panel based upon the crystal structure [27]. The positively charged residues after the TM segment 1 and conserved residues are indicated at the top in italics. The ND motif indicated is a distinctive feature of the CPA1 subfamily whereas the DD motif (NhaP, NhaA) is a distinctive feature of the CPA2 subfamily. The conserved Phe in TM 10 and positively charged residue in TM 11 are shown. Similarly TM 13 has a conserved Thr (or Ser) at the center of the helix. The figure was prepared with the help of Espript server (http://espript.ibcp.fr/ESPript/ESPript/). Conserved residues from the sequence alignment are indicated

initially examined with varying length of the C-terminal tail. The approximate length of the various constructs is shown in Fig. 2, which also illustrates a putative topological model of SOS1.

Initial experiments were focused on the expression of the various lengths of SOS1 in the sod2::ura4 *S. pombe* strain that is devoid of its principle salt tolerance protein sod2. We expressed full-length SOS1 fused to GFP, medium length (fused at amino acid 781 to GFP), and a short version of SOS1 (fused at amino acid 481 to GFP). Figure 3a shows their expression by Western blotting against the GFP tag on each protein. Sod2 fused to GFP was used as a positive control. Sod2 gave an immunoreactive band of approximately 75 kDa, similar to results shown earlier [12]. The three SOS1 constructs have immunoreactive species that were approximately 70, 112, and 152 kDa in size. There were also several smaller immunoreactive bands, which are likely degradation products of the full size protein. We found that the amount of degradation products was very dependent on sample preparation and was increased in the absence of protease inhibitors or if the sample was allowed to warm prior to membrane fractionation (not shown). The knockout strain of sod2::ura4, which did not contain a GFP, tagged protein, did not show any immunoreactive species beyond a slight background staining. While the majority of SOS1s protein was of large size, this was not true for SOS1m and SOS1L. As degradation was occurring during sample preparation, it was unclear if the full-length SOS1m and SOS1L proteins were the majority of species in vivo.

We next characterized the mobility of the SOS1 and sod2 protein in SDS-PAGE (Fig. 3b). Western blotting was against the GFP tag present on the tail of the SOS1 protein or on the sod2 protein (described in [23]). Figure 3b illustrates that neither the SOS1 s (short SOS1 protein) nor sod2, exhibited a mobility shift dependent on reducing conditions. In contrast, the SOS1L protein (Fig. 3c) showed marked changes in mobility. In reducing conditions, the protein was present as a band of approximately

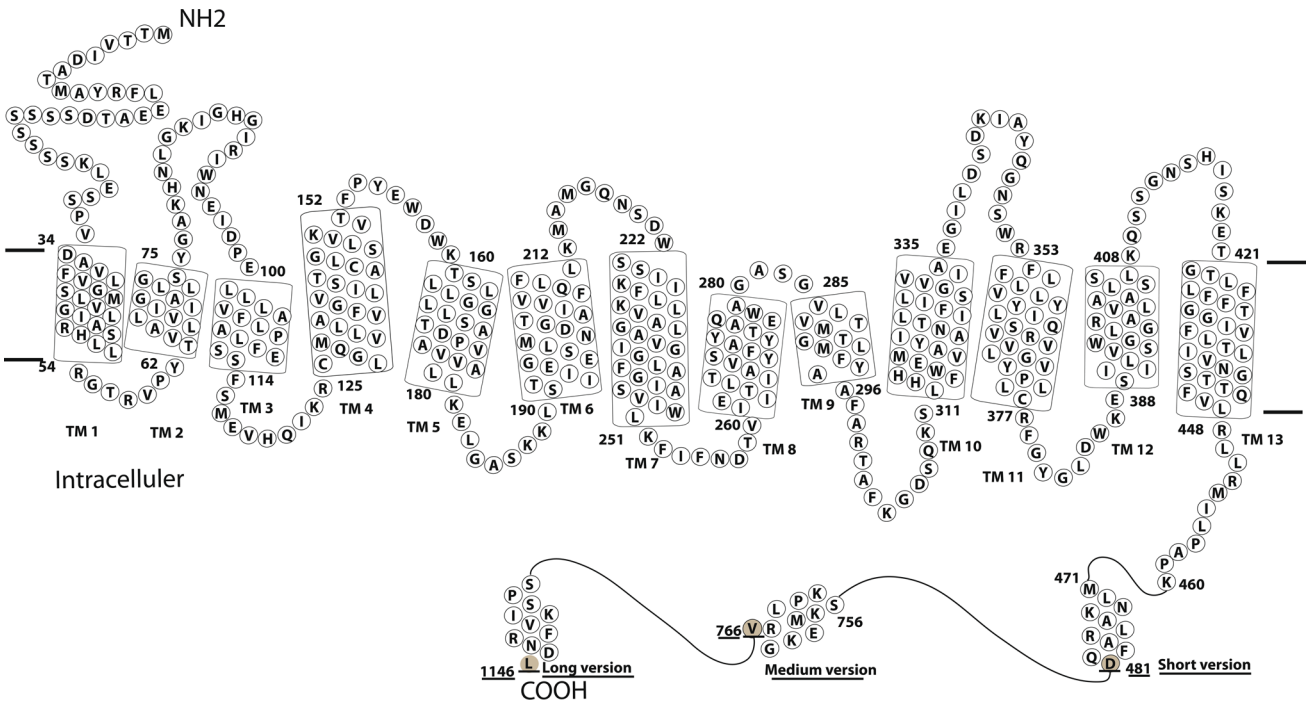

Fig. 2 Predicted topology of SOS1. Predicted topology diagram of *at*SOS1 based on the analysis is shown in Fig. 1. The amino acid numbers of the starting and ending TM segments are indicated. The location of the constructs made for expression is indicated for short (S, 481), medium (M, 766), and full-length (1146, L) SOS1. The last residue is shaded

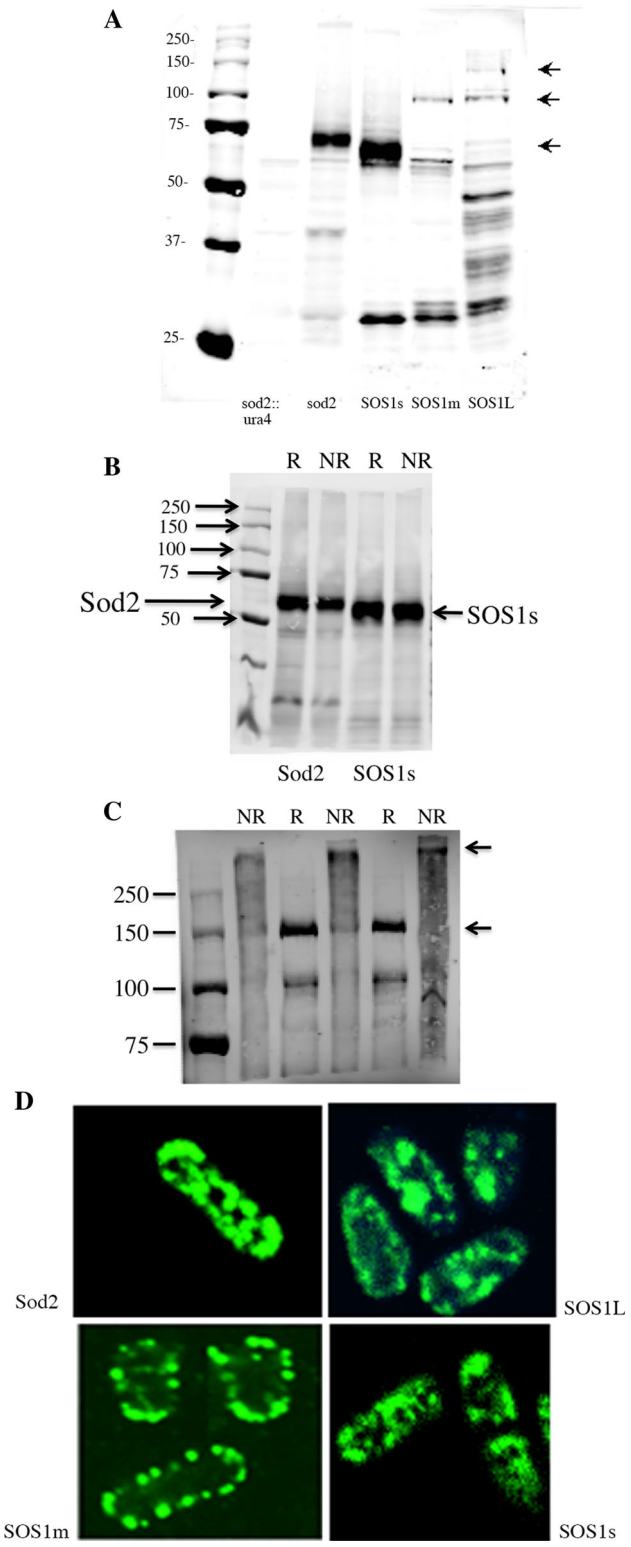

◀**Fig. 3** Expression and characterization of various length SOS1 proteins. **a** Western blot analysis of expression of SOS1 proteins. Cell extracts from *S. pombe* strains expressing either sod2-GFP or various SOS1-GFP constructs (short, s, medium, m, or full-length L) were blotted with anti-GFP antibody as described in the materials and methods. *Arrows* indicate approximate location of full-length SOS1L, SOS1m, and SOS1s proteins, respectively. **b** and **c**, Mobility shifts of SOS1 and sod2 proteins under reducing (R) and non-reducing (NR) conditions. Western blot was with anti-GFP antibody as described in the materials and methods. **b** Western blot of sod2 or SOS1s from 11 % SDS-PAGE transfer. *Arrows* indicate locations of sod2 and SOS1s proteins. **c** Mobility shift of SOSL protein from 9 % SDS-PAGE transfer. *Arrows* indicate location of high and low molecular weight forms. **d** Spinning disk confocal microscopy of SOS1-GFP proteins expressed in *S. pombe*. Exponentially growing cells were harvested and fixed in 4 % formaldehyde, then washed and mounted on coverslips before imaging. Sod2 refers to the wild-type sod2 protein also fused to GFP, mutant SOS1 proteins (full-length, L, medium, m, and short, s) are shown as indicated

150 kDa. In non-reducing conditions, the 150 kDa band was absent and a higher molecular weight band was detected, greater than 250 kDa.

Figure 3d illustrates the localization of the GFP-fused membrane transporters in *S. pombe*. Expression of wild-type sod2 resulted in a localization that was mainly at the plasma membrane. The distribution throughout the plasma membrane was not even, and there were significant amounts of intracellular protein as reported earlier [12]. The SOS1 s and SOS1 proteins gave distributions that were similar to that of sod2, predominantly on the membrane, but also with some evidence of intracellular localization. The SOS1L protein gave a predominantly intracellular localization, with some protein near the cell surface, but much distributed throughout the cytosol or in a perinuclear localization.

We next examined the ability of the various SOS1 proteins to rescue salt tolerance in *S. pombe,* which has the sod2::ura4 mutation. Both LiCl and NaCl are transported by sod2 and other Na^+/H^+ exchangers [11]. LiCl was used for assays in liquid media since it is toxic at lower concentrations, avoiding the osmotic challenge of high concentrations of NaCl. Figure 4 shows the growth of various *S. pombe* lines in liquid media when containing either the SOS1s protein or the sod2 protein. The sod2::ura4 yeast strain was sensitive to LiCl concentrations above 2 mM and to NaCl concentrations above 0.2 M. Growth was intermediate in 0.3 M NaCl and 3 mM LiCl. The sod2 protein rescued growth even in LiCl and NaCl concentrations of 5 mM and 0.5 M, respectively. The SOS1s protein showed intermediate salt tolerance. With exposure to concentrations of 3 mM LiCl salt tolerance was improved. With 4 and 5 mM LiCl there were minor improvements in salt tolerance. In NaCl containing medium, growth was improved with the SOS1 containing cells with 0.3–0.5 mM NaCl. With 0.3 M NaCl, growth was much improved in the SOS1s strain. Growth of the SOS1L and SOS1m strains was compromised and weak relative to SOS1s (not shown).

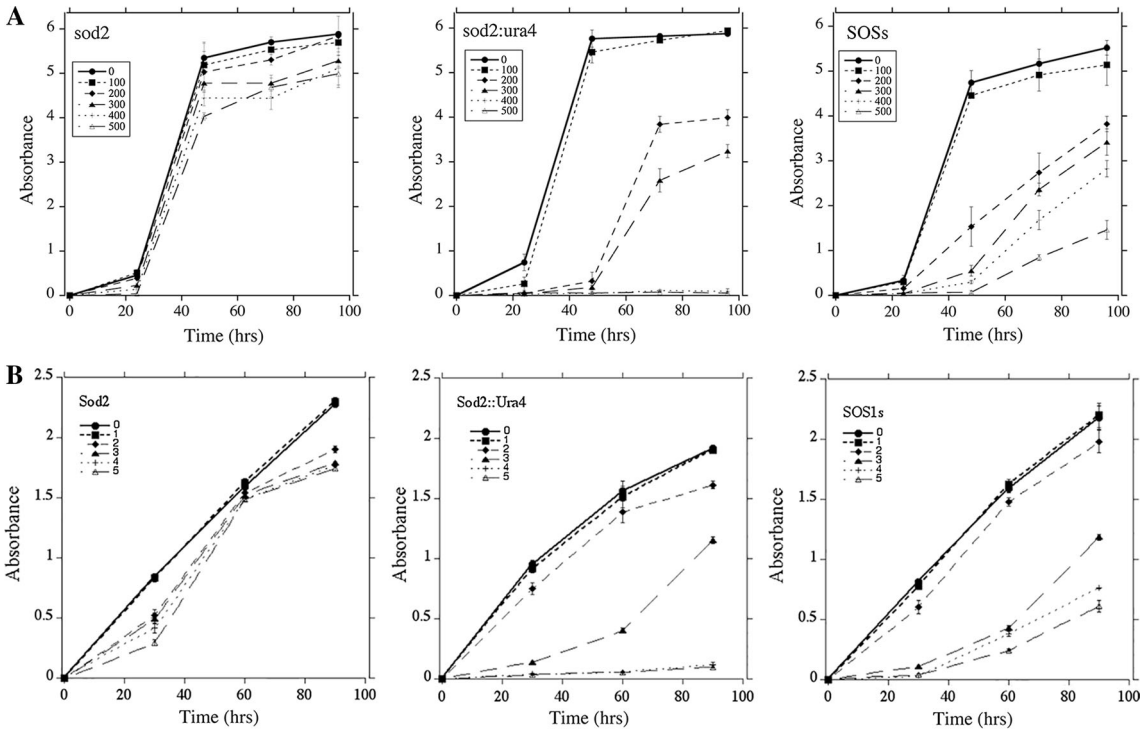

Fig. 4 Growth in liquid medium of *S. pombe* containing either wild-type sod2 or SOS1s protein. LiCl or NaCl tolerance of strains was assessed by inoculating 2×10^6 cells into 2.5 ml of medium at 30 °C for up to 90 h. Growth was assessed by measuring the absorbance of the cell suspensions at 600 nm at the times indicated. Results are the mean ± SE of at least three determinations. *S. pombe* were grown in the presence of 0, 1, 2, 3, 4, or 5 mM LiCl or 0, 0.1, 0.2, 0.3, 0.4, or 0.5 M NaCl as indicated. **a** Comparison of growth rates in NaCl medium of control, *Sod2::ura4 cells, S. pombe* containing sod2 and *S. pombe* containing various SOS1 proteins (full-length, L, medium, m, and short, s). **b** As in A except in various LiCl containing medium as indicated. *Sod2::ura4* refers to *S. pombe* with the sod2 knockout described earlier [11]

We examined the yeast strains growth on solid medium with varying concentrations of LiCl or NaCl. Figure 5 illustrates the results. Cells containing wild-type sod2 grew well in LiCl and NaCl containing media while the *sod2::ura4* knockout strain only showed limited growth when the highest amount of cells were inoculated on medium with higher salt concentrations (4–5 mM LiCl, 400–500 mM NaCl). Expression of SOS1s conveyed limited salt tolerance in both LiCl and NaCl containing medium. In 4 or 5 mM LiCl, SOS1s containing cells grew much better than Sod2::ura4 *S. pombe*, though not as well as cells expressing sod2 protein. The same trend occurred with NaCl concentrations of 300–500 mM.

To further demonstrate that SOS1s directly affects ion flux in *S. pombe*, we examined the expulsion of intracellular Na^+ content as an indication of SOS1s activity. It was previously demonstrated [9, 15] that sod2 accounts for most of Na^+ and Li^+ expulsion in *S. pombe* and its deletion or inactivity in the sod2::ura4 mutant results in greatly reduced expulsion of these ions from the cytosol. We examined the decreasing content of Na^+ after a period of cation loading. The results are shown in Fig. 6. After incubation in NaCl containing medium, Na^+ content of *S. pombe* expressing wild-type sod2 declined relatively rapid. Content of Na^+ in SOS1s-transformed *S. pombe* also declined, though not as rapidly as with sod2. In contrast the Na^+ content of the sod2::ura4 strain was relatively stable over this time period.

Discussion

SOS1 topology

In this report we examine the predicted topology and characterize the salt tolerance protein SOS1. Figures 1 and 2 illustrate the analysis of the structure of SOS1 based on hydrophobicity and structural predictions. SOS1 has a C-terminal regulatory region, which is intracellular [26]. We predicted 13 transmembrane segments, which left residues 1 to 34 as the first N-terminal residues that must be in the extracellular space. By comparison, the existing crystal structures of NHEs reveal two different types of topologies of the N-terminal of the proteins. EcNhaA has 12 transmembrane helices [27] where the N-terminal is intracellular. However, MjNhaP1 and Tth (*Thermus*

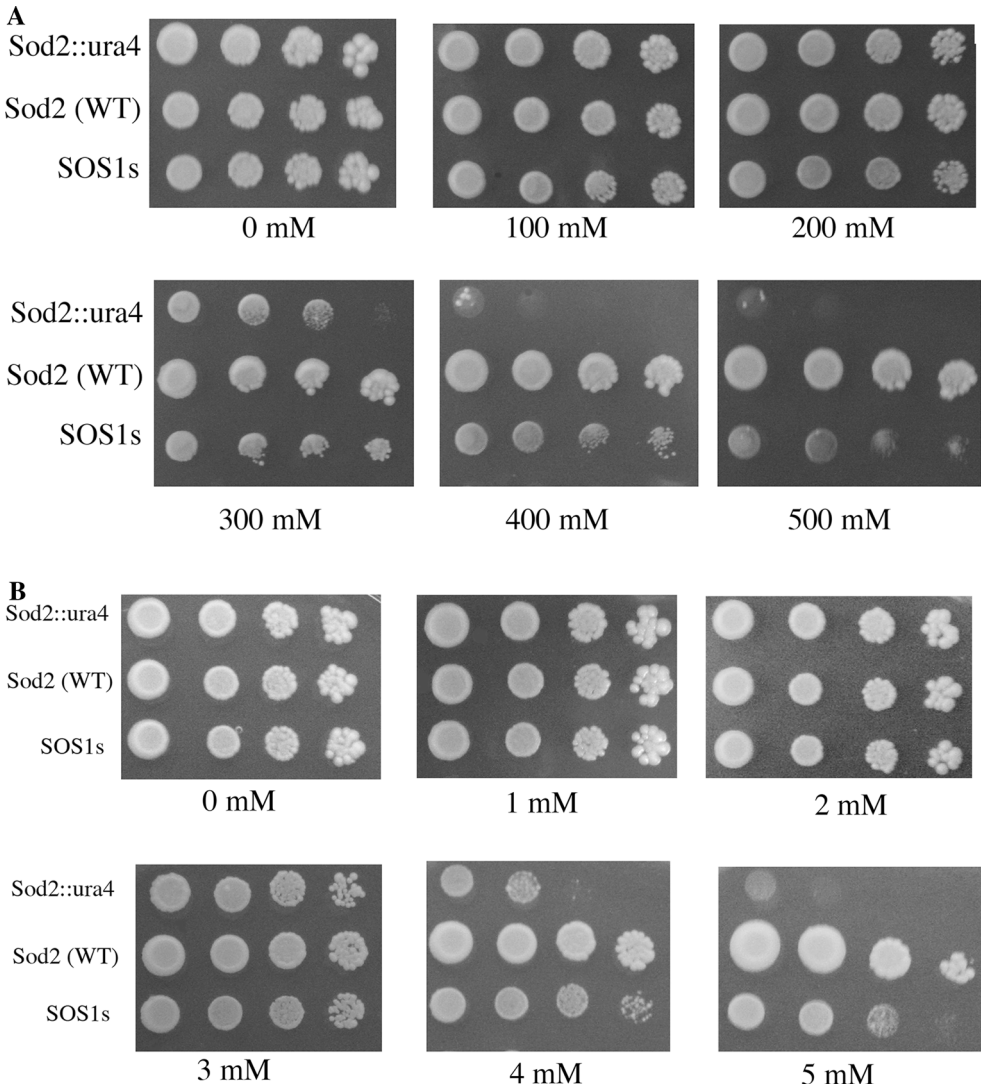

Fig. 5 Growth of wild-type and SOS1 containing *S. pombe* transformants on solid media. Samples of the various yeast strains were taken from stationary phase cultures, were serially diluted 10-fold repeatedly and spotted onto minimal media plates supplemented with NaCl and LiCl at the indicated concentrations. Plates were incubated for 3 days at 30 °C. **a** Panels illustrating growth on plates supplemented with NaCl at the concentrations indicated. **b** Series of panels illustrating growth on plates supplemented with LiCl at the concentrations indicated. Sod2::ura4 refers to *S. pombe* with the sod2 knockout described earlier [11]. WT refers to the sod2::ura4 with sod2 expressed from pREP-41 sod2GFP as described earlier [21]. Other designation refers to SOS1s expressed from pREP-41sod2GFP. Results are typical of at least 3 experiments

thermophilus) NapA have 13 transmembrane helices where the N-terminal is extracellular [28, 29]. Thus the placement of the N-terminus of SOS1 extracellularly, is not unprecedented. It is interesting to note that TM 1 of SOS1 aligned with TM 2 of NHE1 [25], the human Na^+/H^+ exchanger. While NHE1 has been shown to have a cytosolic N-terminus, TM2 of NHE1 would be oriented in the same direction as the proposed orientation of TM 1 of SOS1.

Hydrophobicity analysis and secondary structure prediction identified the first TM segment in SOS1 as 36–54. The downstream sequence is composed of the positively charged containing sequence 55RGTR58 (Fig. 1). Sequence alignment result shows that the region contains at least one positively charged residue in case of both MjNhaP1 and TthNapA [28, 29] whereas in EcNhaA, no positively charged residue is present in this region (Fig. 1), [27]. According to the positive inside rule of the membrane proteins, this kind of region has high propensity to be inside the cell [30] thus supporting the argument for the placement of the N-terminus outside the membrane.

The second TM segment was amino acids 62–75 which have a strong hydrophobicity score and helical prediction. In NhaA, the corresponding region is a beta hairpin that aids in dimerization of the protein. SOS1 possibly possesses membrane-embedded helix at this position. A recent CryoEM structure of SOS1 suggests the dimerization in SOS1 that occurs via both the membrane domain and the cytosolic domain [31]. We examined the dimerization of SOS1 in SDS-PAGE (Fig. 3b). We found that dimerization was sulfhydryl dependent and was dependent on the presence of an intact cytosolic tail of SOS1. The shortened version of the protein was not present as a dimer. The results are not inconsistent with a role of the membrane domain in dimerization in vivo, as this could be masked by the SDS present during electrophoresis. Nevertheless, they

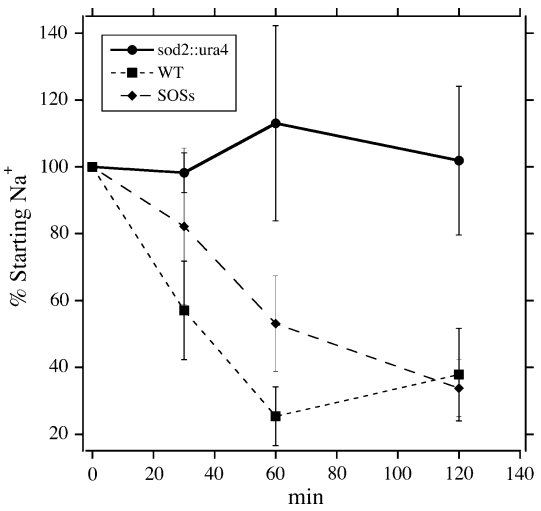

Fig. 6 Loss of Na^+ content from *S. pombe* containing wild-type sod2 or SOS1s protein or the sod2::ura4 knockout strain. Cells were incubated in high NaCl containing medium for 1 h and resuspended in Na^+ free medium. The Na^+ content was determined by atomic absorption spectrophotometry as described in the "Materials and Methods" section. Results are from at least three experiments

are the first demonstration that cysteines present in the cytosolic tail can play a significant role in this regard.

The amino acids 100–114 have a week hydrophobicity score but have a strong helix prediction and are predicted to form TM 3. Predicted TM 4 consists of the residues 125–152.

TM 5 (160–180) of SOS1 may be critical in ion transport. It contains a DPV sequence motif that is conserved in *E. coli* TM 4 and human NHE1 TM 6 [27, 32]. It was also present in sod2 and was important in its function [23, 33].

TM 6 contains the residues 190–212 possessing an As n followed by an Asp(200ND201) motif [34]. The Asp residue is highly conserved. In *E. coli*, the corresponding sequence is Asp163 and Asp164. Mutation of either of these residues results in an inactive protein [35]. This sequence has been proposed to be part of the ion binding and transport site of CPA2 (cation proton antiporter type 2) antiporters [27, 36, 37]. In contrast, in CPA1-type antiporters it is suggested that the ND sequence is a replacement for the DD sequence [37, 38]. This supports the placement of SOS1 in the CPA1 family [39].

TM 7 and TM 8 include residues 222–251 and 260–280, respectively. Corresponding TM segments in EcNhaA (TM 6 and TM 7) have recently been shown to be dispensable for the activity but not for the dimerization [40].

TM 9 is the smallest of all the predicted TM helices containing residues 285–296 while residues 311–335 belong to the TM 10 and contain the conserved Phe. TM 11 is made up of the residues 353–377 containing the conserved positively charge residue Arg365. TM 12 is assigned to residues 388–408. Gly398 is a conserved residue in this TM segment. TM 13 has the residues 421–448 which contain a conserved Thr436 (or Ser) in the middle of this TM segment.

Overall our results present a detailed predicted in silico analysis of SOS1. While Nunez-Ramirez [31] have suggested that SOS1 might have 13 transmembrane segments, no details of these segments and their location and boundaries have been reported. This is the first detailed predicted topology of SOS1 and presents a model subject to future testing.

SOS1 expression

SOS1 has a huge regulatory cytoplasmic tail of approximately 766 amino acids. The tail has been shown to be an important regulator of the membrane domain, and includes an autoinhibitory domain [26]. In this study we examined the ability of SOS1 to rescue salt tolerance in the *S. pombe* strain sod2::ura4. We expressed the protein in *S. pombe* which had its own salt tolerance protein, sod2, deleted. Initial experiments assessed the ability of various SOS1 constructs to rescue salt tolerance and examined the protein expression levels and targeting. In the absence of NaCl or LiCl, the growth of SOS1 containing cells was not different from that of the sod2::ura4 cells. In contrast, SOS1 containing cells could grow and survive on 500 mM NaCl and 5 mM LiCl suggesting that SOS1 can complement salt tolerance in this species. This was verified by atomic absorption spectrophotometry results that showed decreased sodium content. Our shortest SOS1s construct was terminated at amino acid 481. The next longest SOS1m was terminated at amino acid 766. We also expressed SOS1L, the full-length protein (Fig. 2). We found that both SOS1m and SOS1L were subjected to degradation and that they did not complement back salt tolerance very well. Our SOS1s construct was terminated prior to an autoinhibitory domain present on the SOS1 tail [26]. This should have resulted in activation of the SOS1 protein that may have accounted for some of the protective effects demonstrated by the SOS1 s construct. A surprising finding was that the larger constructs of SOS1 were prone to degradation. Whether this occurred in vivo or in the processing of the membrane samples was not clear though it was evident that some further degradation could occur during processing (not shown).

Upon Western blotting against the SOS1 GFP tag, we found that only SOS1L produced a higher molecular weight species, this was presumably a dimer. We suggest that this could be due to intramolecular dimerization of the C-terminal tails of SOS1 through cysteine residues. This could be an important feature of SOS1 structure and function and is the first demonstration of the role of the SOS1 tail in this regard. In the case of the mammalian

Na^+/H^+ exchanger NHE1 sulfhydryl-dependent dimerization has also been reported [41] and NHE1 has also been demonstrated to be present as a dimer [42]. The *E. coli* Na^+/H^+ antiporter also dimerizes and the dimerization has been suggested to be via a beta hairpin on the periplasmic side of the membrane. Deletion of this region results in a monomeric form that is fully functional, but not as efficient as the dimeric native protein under stressful conditions [43]. Dimerization of Na^+/H^+ exchangers may be critical in controlling, or fine tuning their activity [44, 45].

Schizosaccharomyces pombe is an attractive host for the introduction and characterization of salt tolerance proteins from the point of view that deletion of only one protein, results in a salt-sensitive phenotype. This means that introduction of replacement Na^+/H^+ antiporters for sod2 gives unambiguous results. In this study we have found that SOS1 complements the deletion of sod2 in *S. pombe*. Nevertheless, we also found that the extended cytoplasmic domain of SOS1 was subject to proteolytic degradation. Future experiments will explore the use of protease-deficient strains for production of protease-sensitive Na^+/H^+ exchanger proteins in *S. pombe* [46].

Our analysis of the topology of SOS1 suggests that it may have more in common with the proteins MjNhaP1 and TthNapA rather than EcNhaA. Thus it was of interest that it can be expressed and at least partially, complement sod2 function. Sod2 is classified in the CPA2 family of antiporters as opposed to the CPA1 family for SOS1 [39]. Nevertheless, sod2 and SOS1 have 31 % identity and a number of critical regions are preserved (Fig. 1). The topology of sod2 has also not been proven and could be similar to that of SOS1. Further experimentation is necessary to identify amino acids critical in SOS1 function and to confirm the topology of the protein.

Acknowledgments This work was supported by a grant from NSERC to LF. Debajyoti Dutta was partially supported by an NSERC Create grant to the International Research Training Group.

References

1. Wang W, Vinocur B, Altman A (2003) Plant responses to drought, salinity and extreme temperatures: towards genetic engineering for stress tolerance. Planta 218:1–14
2. Yamaguchi T, Blumwald E (2005) Developing salt-tolerant crop plants: challenges and opportunities. Trends Plant Sci 10:615–620
3. Gaxiola RA, Rao R, Sherman A, Grisafi P, Alper SL, Fink GR (1999) The *Arabidopsis thaliana* proton transporters, AtNhx1 and Avp1, can function in cation detoxification in yeast. Proc Natl Acad Sci USA 96:1480–1485
4. Shi H, Ishitani M, Kim C, Zhu JK (2000) The *Arabidopsis thaliana* salt tolerance gene SOS1 encodes a putative Na^+/H^+ antiporter. PNAS USA 97:6896–6901
5. Fukuda A, Nakamura A, Tanaka Y (1999) Molecular cloning and expression of the Na^+/H^+ exchanger gene in *Oryza sativa*. Biochim Biophys Acta 1446:149–155
6. Hamada A, Shono M, Xia T, Ohta M, Hayashi Y, Tanaka A, Hayakawa T (2001) Isolation and characterization of a Na^+/H^+ antiporter gene from the halophyte *Atriplex gmelini*. Plant Mol Biol 46:35–42
7. Chauhan S, Forsthoefel N, Ran Y, Quigley F, Nelson DE, Bohnert HJ (2000) Na^+/myo-inositol symporters and Na^+/H^+-antiport in *Mesembryanthemum crystallinum*. Plant J 24:511–522
8. Shi H, Lee BH, Wu SJ, Zhu JK (2003) Overexpression of a plasma membrane Na^+/H^+ antiporter gene improves salt tolerance in *Arabidopsis thaliana*. Nat Biotechnol 21:81–85
9. Jia Z-P, McCullough N, Martel R, Hemmingsen S, Young PG (1992) Gene amplification at a locus encoding a putative Na^+/H^+ antiporter confers sodium and lithium tolerance in fission yeast. EMBO J 11:1631–1640
10. Haworth RS, Lemire BD, Cragoe EJJ, Fliegel L (1991) Characterization of proton fluxes across the cytoplasmic membrane of the yeast *Saccharomyces cerevisiae*. Biochim Biophys Acta 1098:79–89
11. Dibrov P, Young PG, Fliegel L (1998) Functional analysis of amino acid residues essential for activity in the Na^+/H^+ exchanger of fission yeast. Biochemistry 36:8282–8288
12. Ndayizeye M, Touret N, Fliegel L (2009) Proline 146 is critical to the structure, function and targeting of sod2, the Na^+/H^+ exchanger of *Schizosaccharomyces pombe*. Biochim Biophys Acta 1788:983–992. doi:10.1016/j.bbamem.2009.01.001
13. Quintero FJ, Blatt MR, Pardo JM (2000) Functional conservation between yeast and plant endosomal $Na(^+)/H(^+)$ antiporters. FEBS Lett 471:224–228
14. Gao X, Ren Z, Zhao Y, Zhang H (2003) Overexpression of SOD2 increases salt tolerance of *Arabidopsis*. Plant Physiol 133:1873–1881
15. Dibrov P, Fliegel L (1998) Comparative molecular analysis of Na^+/H^+ exchangers: a unified model for Na^+/H^+ antiport? FEBS Lett 424:1–5
16. Katoh K, Standley DM (2013) MAFFT multiple sequence alignment software version 7: improvements in performance and usability. Mol Biol Evol 30:772–780. doi:10.1093/molbev/mst010
17. Buchan DW, Minneci F, Nugent TC, Bryson K, Jones DT (2013) Scalable web services for the PSIPRED protein analysis workbench. Nucleic Acids Res 41:W349–W357. doi:10.1093/nar/gkt381
18. Kloczkowski A, Ting KL, Jernigan RL, Garnier J (2002) Combining the GOR V algorithm with evolutionary information for protein secondary structure prediction from amino acid sequence. Proteins 49:154–166. doi:10.1002/prot.10181
19. Moller S, Croning MD, Apweiler R (2001) Evaluation of methods for the prediction of membrane spanning regions. Bioinformatics 17:646–653
20. Hofmann K, Stoffel W (1993) TMBASE—a database of membrane spanning protein segments. Biol Chem Hoppe-Seyler 374:166
21. Fliegel L, Wiebe C, Chua G, Young PG (2005) Functional expression and cellular localization of the Na^+/H^+ exchanger Sod2 of the fission yeast *Schizosaccharomyces pombe*. Can J Physiol Pharmacol 83:565–572
22. Slepkov ER, Chow S, Lemieux MJ, Fliegel L (2004) Proline residues in transmembrane segment IV are critical for activity, expression and targeting of the Na^+/H^+ exchanger isoform 1. Biochem J 379:31–38
23. Ullah A, Kemp G, Lee B, Alves C, Young H, Sykes BD, Fliegel L (2013) Structural and functional analysis of transmembrane segment IV of the salt tolerance protein Sod2. J Biol Chem 288:24609–24624. doi:10.1074/jbc.M113.483065

24. Wakabayashi S, Pang T, Su X, Shigekawa M (2000) A novel topology model of the human Na^+/H^+ exchanger isoform 1. J Biol Chem 275:7942–7949
25. Liu Y, Basu A, Li X, Fliegel L (2015) Topological analysis of the Na/H exchanger. Biochim Biophys Acta 1848:2385–2393. doi:10.1016/j.bbamem.2015.07.011
26. Quintero FJ, Martinez-Atienza J, Villalta I, Jiang X, Kim WY, Ali Z, Fujii H, Mendoza I, Yun DJ, Zhu JK, Pardo JM (2011) Activation of the plasma membrane Na/H antiporter salt-overly-sensitive 1 (SOS1) by phosphorylation of an auto-inhibitory C-terminal domain. Proc Natl Acad Sci USA 108:2611–2616. doi:10.1073/pnas.1018921108
27. Hunte C, Screpanti E, Venturi M, Rimon A, Padan E, Michel H (2005) Structure of a Na^+/H^+ antiporter and insights into mechanism of action and regulation by pH. Nature 435:1197–1202
28. Goswami P, Paulino C, Hizlan D, Vonck J, Yildiz O, Kuhlbrandt W (2011) Structure of the archaeal Na^+/H^+ antiporter NhaP1 and functional role of transmembrane helix 1. EMBO J 30:439–449. doi:10.1038/emboj.2010.321
29. Lee C, Kang HJ, von Ballmoos C, Newstead S, Uzdavinys P, Dotson DL, Iwata S, Beckstein O, Cameron AD, Drew D (2013) A two-domain elevator mechanism for sodium/proton antiport. Nature 501:573–577. doi:10.1038/nature12484
30. von Heijne G (2006) Membrane–protein topology. Nat Rev Mol Cell Biol 7:909–918. doi:10.1038/nrm2063
31. Nunez-Ramirez R, Sanchez-Barrena MJ, Villalta I, Vega JF, Pardo JM, Quintero FJ, Martinez-Salazar J, Albert A (2012) Structural insights on the plant salt-overly-sensitive 1 (SOS1) $Na(^+)/H(^+)$ antiporter. J Mol Biol 424:283–294. doi:10.1016/j.jmb.2012.09.015
32. Tzeng J, Lee BL, Sykes BD, Fliegel L (2010) Structural and functional analysis of transmembrane segment VI of the NHE1 isoform of the Na^+/H^+ exchanger. J Biol Chem 285:36656–36665. doi:10.1074/jbc.M110.161471
33. Fliegel L (2005) Identification of conserved polar residues important for salt tolerance by the Na^+/H^+ exchanger of *Schizosaccharomyces pombe*. Mol Cell Biochem 268:83–92
34. Wohlert D, Kuhlbrandt W, Yildiz O (2014) Structure and substrate ion binding in the sodium/proton antiporter PaNhaP. Elife 3:e03579. doi:10.7554/eLife.03579
35. Inoue H, Noumi T, Tsuchiya T, Kanazawa H (1995) Essential aspartic acid residues, Asp-133, Asp-163 and Asp-164, in the transmembrane helices of a Na^+/H^+ antiporter (NhaA) from *Escherichia coli*. FEBS Lett 363:264–268
36. Maes M, Rimon A, Kozachkov-Magrisso L, Friedler A, Padan E (2012) Revealing the ligand binding site of NhaA Na^+/H^+ antiporter and its pH dependence. J Biol Chem 287:38150–38157. doi:10.1074/jbc.M112.391128
37. Paulino C, Kuhlbrandt W (2014) pH- and sodium-induced changes in a sodium/proton antiporter. Elife 3:e01412. doi:10.7554/eLife.01412
38. Hellmer J, Teubner A, Zeilinger C (2003) Conserved arginine and aspartate residues are critical for function of MjNhaP1, a Na^+/H^+ antiporter of *M. jannaschii*. FEBS Lett 542:32–36
39. Brett CL, Donowitz M, Rao R (2005) Evolutionary origins of eukaryotic sodium/proton exchangers. Am J Physiol Cell Physiol 288:C223–C239
40. Padan E, Danieli T, Keren Y, Alkoby D, Masrati G, Haliloglu T, Ben-Tal N, Rimon A (2015) NhaA antiporter functions using 10 helices, and an additional 2 contribute to assembly/stability. Proc Natl Acad Sci USA 112:E5575–E5582. doi:10.1073/pnas.1510964112
41. Fliegel L, Haworth RS, Dyck JRB (1993) Characterization of the placental brush border membrane Na^+/H^+ exchanger: identification of thiol-dependent transitions in apparent molecular size. Biochem J 289:101–107
42. Moncoq K, Kemp G, Li X, Fliegel L, Young HS (2008) Dimeric structure of human Na^+/H^+ exchanger isoform 1 overproduced in *Saccharomyces cerevisiae*. J Biol Chem 283:4145–4154
43. Rimon A, Tzubery T, Padan E (2007) Monomers of the NhaA Na +/H + antiporter of Escherichia coli are fully functional yet dimers are beneficial under extreme stress conditions at alkaline pH in the presence of Na + or Li+. J Biol Chem 282:26810–26821. doi:10.1074/jbc.M704469200
44. Hisamitsu T, Pang T, Shigekawa M, Wakabayashi S (2004) Dimeric interaction between the cytoplasmic domains of the Na^+/H^+ exchanger NHE1 revealed by symmetrical intermolecular cross-linking and selective co-immunoprecipitation. Biochemistry 43:11135–11143
45. Hendus-Altenburger R, Kragelund BB, Pedersen SF (2014) Structural dynamics and regulation of the mammalian SLC9A family of $Na(^+)/H(^+)$ exchangers. Curr Top Membr 73:69–148. doi:10.1016/B978-0-12-800223-0.00002-5
46. Idiris A, Bi K, Tohda H, Kumagai H, Giga-Hama Y (2006) Construction of a protease-deficient strain set for the fission yeast *Schizosaccharomyces pombe*, useful for effective production of protease-sensitive heterologous proteins. Yeast 23:83–99. doi:10.1002/yea.1342